

## Supplementary Data

### Supplementary Materials and Methods

#### Polymer synthesis and functionalization with cell-adhesive peptides

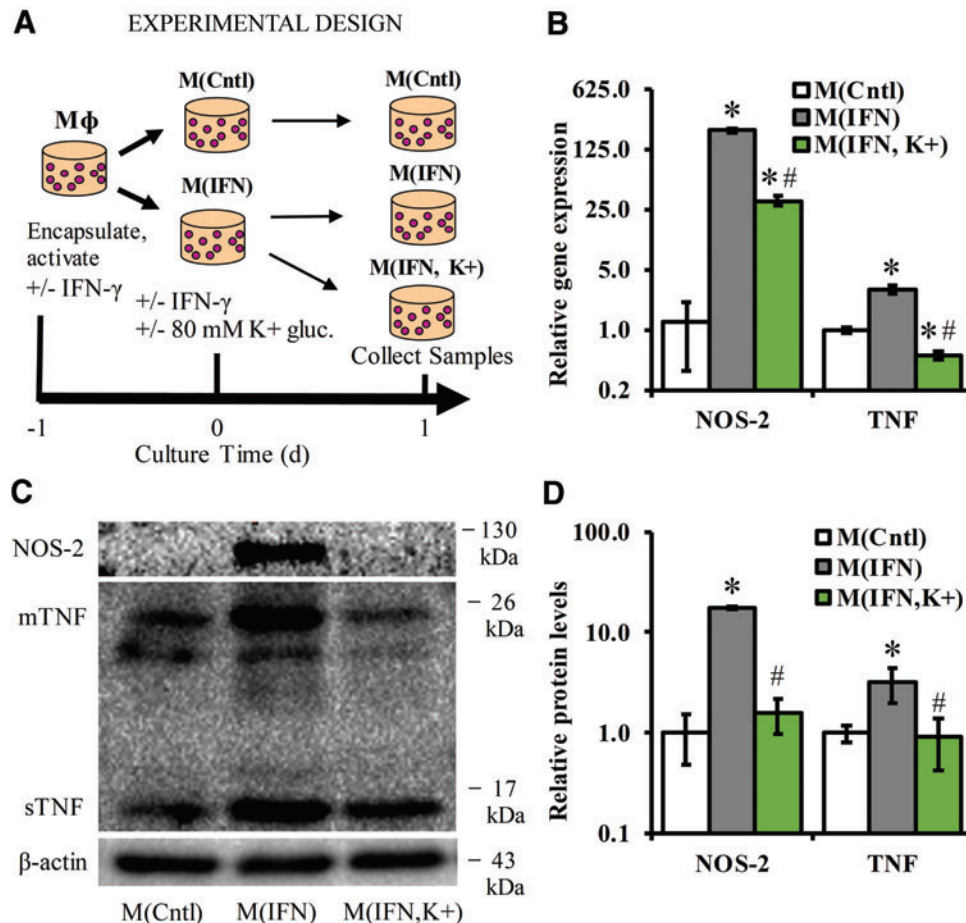
Poly(ethylene glycol) diacrylate (PEGDA) was synthesized from PEG-diol (6 kDa; Sigma Aldrich) at ~99% acrylation as reported previously.<sup>S1</sup> Concurrently, NH<sub>2</sub>-Arg-Gly-Asp-Ser-COOH (RGDS; American Peptide Company) was reacted with 3.4 kDa acryloyl-PEG-succinimidyl valerate (ACRL-PEG-NHS; Laysan Bio) at a 1:3 molar ratio for 2 h in 50 mM sodium bicarbonate buffer (pH 8.5). RGDS was included to facilitate cell attachment within the PEGDA network. The product (ACRL-PEG-RGDS) was purified by dialysis, lyophilized, and stored at -80°C until further use.

#### Cell culture and encapsulation

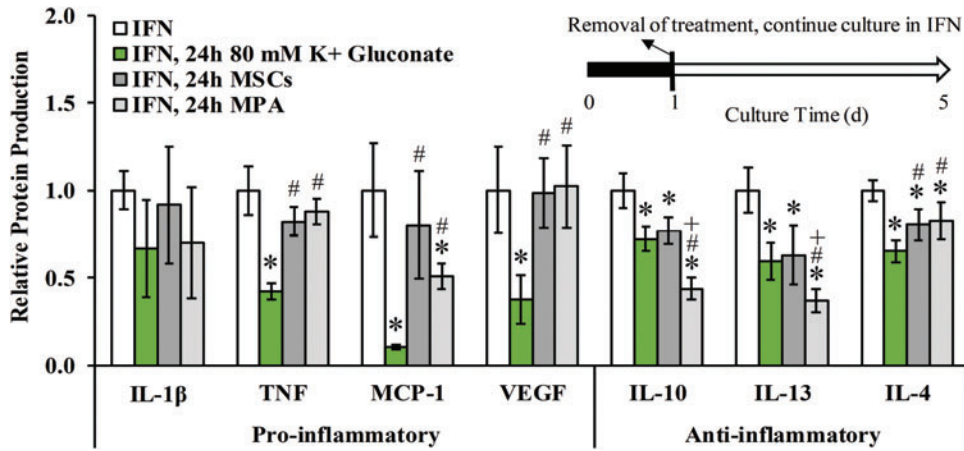
Raw 264.7 murine macrophages (a cell line) were thawed and expanded in regular growth medium: high-glucose Dulbecco's modified Eagle's medium (DMEM; Corning) supplemented with 10% fetal bovine serum (FBS; Hyclone,

Atlanta Biologicals, Inc.). Primary human OACs (Cell Applications, Inc.) were expanded in chondrogenic growth media for four passages, transitioned into regular growth medium for 1 passage, and utilized at passage 5, as described previously.<sup>S2</sup> The OAC donor at this passage has been previously demonstrated to respond to activated Raw 264.7 macrophages in a manner consistent with early OA<sup>2</sup> and exhibits increased production of matrix metalloproteinases (MMPs) and proinflammatory cytokines relative to chondrocytes isolated from a patient without OA.<sup>2</sup>

Bone marrow-derived human mesenchymal stem cells (hMSCs) were obtained as passage 1 in a cryovial from Texas A&M Institute for Regenerative Medicine. Cells were thawed and expanded in Minimum Essential Medium  $\alpha$  (MEM $\alpha$ ; Gibco) supplemented with 16.5% FBS (Atlanta Biologicals) and utilized at passage 4. These cells have been confirmed by Texas A&M to be CD44<sup>+</sup>, CD105<sup>+</sup>, CD29<sup>+</sup>, CD166<sup>+</sup>, CD14<sup>-</sup>, CD34<sup>-</sup>, and CD45<sup>-</sup> and to undergo adipogenic, chondrogenic, or osteogenic differentiation under inductive culture conditions.



**SUPPLEMENTARY FIG. S1.** (A) Experimental design, including experimental groups, activation parameters, and time course. (B) Relative NOS-2 and TNF gene and (C, D) protein expression in Raw 264.7 M $\Phi$ s after stimulation with/without IFN and 80 mM K<sup>+</sup> gluconate. Both membrane-bound (mTNF) and soluble TNF (sTNF) were utilized for quantification; \* and # denote statistical significance ( $p < 0.05$ ) relative to M(Cntl) and M(IFN), respectively. TNF, tumor necrosis factor.



**SUPPLEMENTARY FIG. S2.** Relative protein production of several proinflammatory and anti-inflammatory molecules in Raw 264.7 MΦs after 5 days in culture. Treatments were applied only during the first day of culture. \*Denotes a significant difference relative to IFN controls. #Denotes a significant difference relative to 24-h 80 mM K<sup>+</sup> gluconate. +Denotes a significant difference relative to 24-h MSCs.

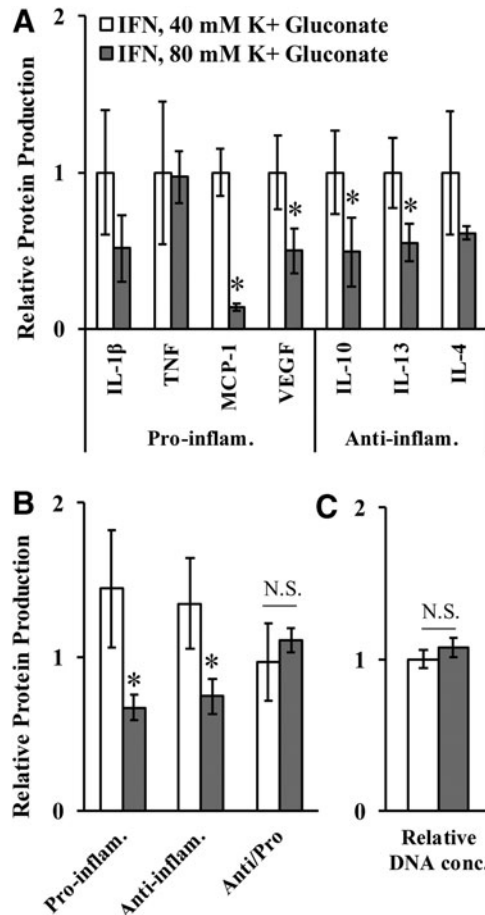
Cell encapsulation was performed as previously described.<sup>S1</sup> Briefly, aliquots (200 μL; 1 × 10<sup>6</sup> cells per construct) of the cell/polymer suspension were dispensed into the wells of a 48-well plate (Corning) and cured by exposure to long-wave UV light (~10 mW/cm<sup>2</sup>) for 6 min. After 24 h of equilibration to the new 3D environment and activation with 75 ng/mL interferon-gamma (IFN; R&D Systems), macrophage discs were placed in culture with or without IFN, K<sup>+</sup> gluconate (Sigma), and methylprednisolone acetate (MPA; Fisher Scientific). At culture end points, the hydrogels were washed in DPBS for 5–10 min, harvested by flash-freezing in liquid nitrogen, and stored at –80°C until further analysis.

### Reverse Transcriptase–Quantitative Polymerase Chain Reaction

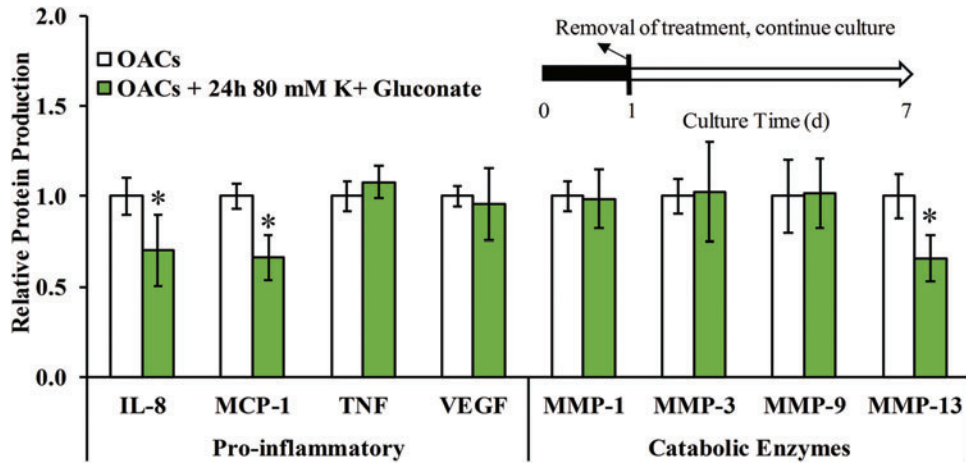
mRNA extraction and quantitative polymerase chain reaction (qPCR) were performed to compare mRNA levels across the various experimental groups as described previously.<sup>S3</sup> Validated qPCR primers were purchased from Qiagen or OriGene. Available primer sequences are provided in Supplementary Table S1. Gene expression was normalized to the combination of three reference genes (GAPDH, L32, and β-actin) and is presented relative to day 1 M(Cntl). The arithmetic mean of three reference genes (instead of one) was utilized because gene expression of a single traditional housekeeping gene often varies significantly among treatment groups and cell types, reducing the accuracy of quantification of the gene of interest. Combining three reference genes is known to be a more robust and accurate method of quantifying differences in mRNA expression among treatment groups.<sup>S4</sup> Melting temperature analysis was performed for each reaction to verify the appropriate amplification product.

### Western blot and MAGPIX immunoassay multiplexing

For the first experiment, western blots were performed under denaturing and reducing conditions with a 12% SDS-PAGE gel as described previously.<sup>S5</sup> Protein levels of NOS-2



**SUPPLEMENTARY FIG. S3.** (A) Relative protein production of proinflammatory and anti-inflammatory molecules in Raw 264.7 MΦs after 5 days in culture. (B) The corresponding pro- and anti-inflammatory profiles and their ratio (Anti/Pro). (C) Relative DNA concentrations of MΦs after 5 days. Treatments were applied continuously during the 5-day culture. \*Denotes a significant difference relative to 40 mM K<sup>+</sup> gluconate. N.S., nonsignificant difference.



**SUPPLEMENTARY FIG. S4.** Relative protein production of several proinflammatory and catabolic enzyme markers in OACs cultured for 7 days. Treatment with 80 mM K<sup>+</sup> gluconate was only applied during the first day of culture. \*Denotes a significant difference relative to unstimulated OAC controls. OACs, osteoarthritic chondrocytes.

and tumor necrosis factor (TNF) (both soluble TNF and membrane-bound TNF) were quantified through integrated band densitometry. For the second experiment, protein levels of TNF, monocyte chemoattractant protein-1 (MCP-1), vascular endothelial growth factor (VEGF), and interleukin (IL) -10, -13, -4, -1 $\beta$ , and -6 were measured from M $\Phi$  cell lysates using a murine magnetic bead analyte kit (EMD Millipore) and the MAGPIX detection system (Luminex) according to manufacturer's protocols. MMP -1, -3, -9, and -13, TNF, VEGF, MCP-1, and interleukin-8 (IL-8) were measured from OAC lysates using a human premixed magnetic bead analyte kit (R&D Systems). With the exception of IL-1 $\beta$ , all of the proteins investigated are secreted conventionally, meaning they are continually processed from the endoplasmic reticulum to the Golgi apparatus and secreted through the plasma membrane. Therefore, for proteins analyzed in the study, it is reasonable to assume that protein levels in the cell lysate are representative of what is secreted. The resulting measures were then normalized by sample DNA content, assessed with the PicoGreen assay as per the manufacturer's instructions (Life Technologies).

Last, these concentrations normalized to DNA content were then further normalized to IFN controls (Fig. 1).

Many studies only examine 1 or 2 pro- or anti-inflammatory markers without considering the cumulative effect of these markers. To offer more insight into the underlying phenomena, we also analyzed and presented the data in a different way (Fig. 1). In this study, all markers belonging to the pro- or anti-inflammatory classification were pooled into a single metric (rather than 3–4 separate proteins for each). For a given marker (i.e., TNF), the concentration determined using MAGPIX was normalized first to DNA concentration and then to the average concentration for that marker (i.e., TNF) across all samples. These normalization steps enable (1) concentrations for a given marker (i.e., TNF) to be expressed on a per cell basis (DNA normalization) and (2) comparison between proteins that are normally expressed at different absolute amounts (i.e., TNF vs. MCP-1). The resulting normalized values for TNF, MCP-1, VEGF, and IL-10, IL-13, and IL-4 were averaged to yield values representing the pro- and anti-inflammatory profiles, respectively. Last, for a given sample, the value for the anti-

**SUPPLEMENTARY TABLE S1. PRIMER SEQUENCES USED FOR QUANTITATIVE REVERSE TRANSCRIPTASE–POLYMERASE CHAIN REACTION ANALYSIS OF GENES ASSOCIATED WITH M(IFN)s**

| Function               | Gene marker    | Primer sequence forward (F), reverse (R)               |
|------------------------|----------------|--|
| Proinflammatory        | NOS-2          | F: GAGACAGGGAAGTCTGAAGCAC<br>R: CCAGCAGTAGTTGCTCCTCTTC |
|                        | TNF            | F: GGTGCCTATGTCTCAGCCTCTT<br>R: GCCATAGAAGTATGAGAGGGAG |
| Reference/Housekeeping | $\beta$ -actin | F: GGCTGTATTCCCCTCATCG<br>R: CCAGTTGGTAACAATGCCATGT    |
|                        | GAPDH          | F: GCAGTGGCAAAGTGGAGATT<br>R: CGCTCCTGGAAGATGGTGAT     |
|                        | L32            | F: ATCAGGCACCAGTCAGACCGAT<br>R: GTTGCTCCCATACCGATGTTGG |

inflammatory profile was divided by the value for the proinflammatory profile to yield the anti/proinflammatory ratio. A strength of this method is that it simplifies complex marker-dependent data into a more understandable and relatable format. However, it assumes that the selected cytokines are major contributors to the inflammatory process in OA and that all included proteins have equal weights in terms of their contribution to pro- or anti-inflammatory processes, which may or may not be the case *in vivo*. Pooling data can also be viewed as a weakness because it may overlook the nuance of cell biology. As such, we reasoned that presenting the data in both individual and combined formats was appropriate. That said, it is important to note that pooling markers together is an accepted method of analyzing the macrophage phenotype.<sup>S6–S8</sup> All markers were selected for analyses because of their prevalence in OA and macrophage literature.<sup>S9–S18</sup>

IL-6 is a highly pleiotropic cytokine,<sup>S19–S23</sup> meaning it can exert context-dependent pro- or anti-inflammatory effects depending on a number of factors, including the receptor profile on the receiving cell, presence of other costimulatory signals, and cell type. For this reason, IL-6 was not included in the pooling of data into either the pro- or anti-inflammatory category.

#### Justification of experimental parameters

Three-dimensional culture with PEGDA hydrogels. To improve the relevance of our experiments, PEGDA hydrogels were selected as the material for the 3D *in vitro* model over conventional 2D culture. Furthermore, these materials restrict cell proliferation and protein adhesion even in serum-containing culture environments.<sup>S24–S26</sup> These properties enable tight control over the study of the treatment in question on cell phenotype, without confounding influences from the selection of specific phenotypes over time or due to the presence of adhered proteins. Culture in PEGDA hydrogels also enables the examination of progression of macrophage phenotype over time, without concerns for proliferation and overconfluence noticed in traditional 2D culture wells. In the present studies, we have tethered the peptide RGD to the PEGDA network to enable consistent initial cell–matrix adhesion levels across experimental groups.

Macrophage activation with interferon-gamma. M $\Phi$  activation with IFN was chosen to induce a cell phenotype that represented inflammation in OA. Specifically, M $\Phi$  stimulation with IFN increases the production of several proinflammatory factors (i.e., nitric oxide and TNF)<sup>S27–S29</sup> suggested to underlie OA pathology.<sup>S14,S16,S18</sup> Furthermore, the intracellular pathways elicited in response to IFN are commonly studied/well known and may offer direct insight into mechanisms of K<sup>+</sup> influence in future work.

Concentration and exposure time of K<sup>+</sup> gluconate, MSCs, and MPA. The concentrations of added osmolytes (i.e., 40 and 80 mM K<sup>+</sup> gluconate) and time of exposure (1 day) were selected based on literature from the bioelectricity field.<sup>S30–S34</sup> In addition, they match favorably with the more recent report demonstrating that hyperosmolar extracellular K<sup>+</sup> solutions suppress T cell effector function.<sup>S35</sup> It should be noted that this more recent report (and the few others investigating

K<sup>+</sup> influences in immunology) had not yet been published during the planning of these experiments.

MSCs are a cell therapy currently being investigated in a number of clinical OA trials,<sup>S36,S37</sup> and MPA is a clinically approved corticosteroid commonly used in intra-articular injections.<sup>S38,S39</sup> The 3:1 ratio of MSCs:M $\Phi$  was determined based on estimates of MSC numbers utilized across clinical OA trials<sup>S40</sup> and synovial M $\Phi$  numbers deduced from average synovial volume<sup>S41,S42</sup> and M $\Phi$  cell density in the synovial intima of OA patients.<sup>S43</sup> The concentration of the corticosteroid MPA (0.1 mM) was selected from previous *in vitro* chondrocyte and macrophage literature.<sup>S44–S48</sup>

#### Statistical analyses

All data are reported as mean  $\pm$  standard deviation. Means were compared using a one-way ANOVA ( $n=3–5$  samples per group). All experiments were performed with one MSC and one OAC donor. The assumption for homogeneity of variance was tested utilizing Levene's test. Comparison of experimental group means was performed using Tukey's *post hoc* test or a Games–Howell *post hoc* test (in cases where Levene's test returned a significant result). For all tests, a  $p$ -value  $<0.05$  was considered significant and SPSS software was utilized.

#### Supplementary References

- Erndt-Marino, J.D., and Hahn, M.S. Probing the response of human osteoblasts following exposure to sympathetic neuron-like PC-12 cells in a 3D coculture model. *J Biomed Mater Res A* **105**, 984, 2017.
- Samavedi, S., Diaz-Rodriguez, P., Erndt-Marino, J.D., and Hahn, M.S. A Three-Dimensional Chondrocyte-Macrophage Coculture System to Probe Inflammation in Experimental Osteoarthritis. *Tissue Eng Pt A* **23**, 101, 2017.
- Erndt-Marino, J.D., Jimenez-Vergara, A.C., Diaz-Rodriguez, P., *et al.* In vitro evaluation of a basic fibroblast growth factor-containing hydrogel toward vocal fold lamina propria scar treatment. *J Biomed Mater Res B Appl Biomater* **106**, 1258, 2018.
- Vandesompele, J., De Preter, K., Pattyn, F., *et al.* Accurate normalization of real-time quantitative RT-PCR data by geometric averaging of multiple internal control genes. *Genome Biol* **3**, 2002. DOI: 10.1186/gb-2002-3-7-research0034.
- Erndt-Marino, J.D., Munoz-Pinto, D.J., Samavedi, S., *et al.* Evaluation of the Osteoinductive Capacity of Polydopamine-Coated Poly(epsilon-caprolactone) Diacrylate Shape Memory Foams. *ACS Biomater Sci Eng* **1**, 1220, 2015.
- Utomo, L., van Osch, G.J.V.M., Bayon, Y., Verhaar, J.A.N., and Bastiaansen-Jenniskens, Y.M. Guiding synovial inflammation by macrophage phenotype modulation: an *in vitro* study towards a therapy for osteoarthritis. *Osteoarthritis Cartilage* **24**, 1629, 2016.
- Grotenhuis, N., Bayon, Y., Lange, J.F., Van Osch, G.J.V.M., and Bastiaansen-Jenniskens, Y.M. A culture model to analyze the acute biomaterial-dependent reaction of human primary macrophages. *Biochem Biophys Res Commun* **433**, 115, 2013.
- Boersema, G.S.A., Utomo, L., Bayon, Y., *et al.* Monocyte subsets in blood correlate with obesity related

- response of macrophages to biomaterials in vitro. *Biomaterials* **109**, 32, 2016.
- S9. Aigner, T., Soder, S., Gebhard, P.M., McAlinden, A., and Haag, J. Mechanisms of disease: role of chondrocytes in the pathogenesis of osteoarthritis—structure, chaos and senescence. *Nat Clin Pract Rheumatol* **3**, 391, 2007.
- S10. Berenbaum, F., and van den Berg, W.B. Inflammation in osteoarthritis: changing views. *Osteoarthritis Cartilage* **23**, 1823, 2015.
- S11. Dreier, R. Hypertrophic differentiation of chondrocytes in osteoarthritis: the developmental aspect of degenerative joint disorders. *Arthritis Res Ther* **12**, 216, 2010.
- S12. Gaudi, S.J., Standton, H., Little, C.B., and Fosnang, A.J. *Proteoglycan and Collagen Degradation in Osteoarthritis*. Cartilage: Springer; 2017, p. 41.
- S13. Goldring, M.B., Otero, M., Plumb, D.A., *et al.* Roles of inflammatory and anabolic cytokines in cartilage metabolism: signals and multiple effectors converge upon MMP-13 regulation in osteoarthritis. *Eur Cells Mater* **21**, 202, 2011.
- S14. Kapoor, M., Martel-Pelletier, J., Lajeunesse, D., Pelletier, J.P., and Fahmi, H. Role of proinflammatory cytokines in the pathophysiology of osteoarthritis. *Nat Rev Rheumatol* **7**, 33, 2011.
- S15. Liu-Bryan, R., and Terkeltaub, R. Emerging regulators of the inflammatory process in osteoarthritis. *Nat Rev Rheumatol* **11**, 35, 2015.
- S16. Sellam, J., and Berenbaum, F. The role of synovitis in pathophysiology and clinical symptoms of osteoarthritis. *Nat Rev Rheumatol* **6**, 625, 2010.
- S17. van der Kraan, P.M., and van den Berg, W.B. Chondrocyte hypertrophy and osteoarthritis: role in initiation and progression of cartilage degeneration? *Osteoarthritis Cartilage* **20**, 223, 2012.
- S18. Wojdasiewicz, P., Poniatowski, L.A., and Szukiewicz, D. The role of inflammatory and anti-inflammatory cytokines in the pathogenesis of osteoarthritis. *Mediat Inflamm* **2014**, 561459, 2014.
- S19. Hunter, C.A., and Jones, S.A. IL-6 as a keystone cytokine in health and disease. *Nat Immunol* **16**, 448, 2015.
- S20. Petersen, A.M.W., and Pedersen, B.K. The role of IL-6 in mediating the anti-inflammatory effects of exercise. *J Physiol Pharmacol* **57**, 43, 2006.
- S21. Scheller, J., Chalaris, A., Schmidt-Arras, D., and Rose-John, S. The pro- and anti-inflammatory properties of the cytokine interleukin-6. *Bba-Mol Cell Res* **1813**, 878, 2011.
- S22. Mauer, J., Denson, J.L., and Bruning, J.C. Versatile functions for IL-6 in metabolism and cancer. *Trends Immunol* **36**, 92, 2015.
- S23. Mauer, J., Chaurasia, B., Goldau, J., *et al.* Signaling by IL-6 promotes alternative activation of macrophages to limit endotoxemia and obesity-associated resistance to insulin. *Nat Immunol* **15**, 423, 2014.
- S24. Gombotz, W.R., Guanghui, W., Horbett, T.A., and Hoffman, A.S. Protein adsorption to poly(ethylene oxide) surfaces. *J Biomed Mater Res* **25**, 1547, 1991.
- S25. Williams, C.G., Kim, T.K., Taboas, A., Malik, A., Manson, P., and Elisseff, J. In vitro chondrogenesis of bone marrow-derived mesenchymal stem cells in a photopolymerizing hydrogel. *Tissue Eng* **9**, 679, 2003.
- S26. Nuttelman, C.R., Tripodi, M.C., and Anseth, K.S. Synthetic hydrogel niches that promote hMSC viability. *Matrix Biol* **24**, 208, 2005.
- S27. Murray, H.W., Spitalny, G.L., and Nathan, C.F. Activation of mouse peritoneal macrophages in vitro and in vivo by interferon-gamma. *J Immunol* **134**, 1619, 1985.
- S28. Su, X., Yu, Y., Zhong, Y., *et al.* Interferon-gamma regulates cellular metabolism and mRNA translation to potentiate macrophage activation. *Nat Immunol* **16**, 838, 2015.
- S29. Vila-del Sol, V., Punzon, C., and Fresno, M. IFN-gamma-induced TNF-alpha expression is regulated by interferon regulatory factors 1 and 8 in mouse macrophages. *J Immunol* **181**, 4461, 2008.
- S30. Lan, J.Y., Williams, C., Levin, M., and Black, L.D. Depolarization of cellular resting membrane potential promotes neonatal cardiomyocyte proliferation in vitro. *Cell Mol Bioeng* **7**, 432, 2014.
- S31. Sundelacruz, S., Levin, M., and Kaplan, D.L. Membrane potential controls adipogenic and osteogenic differentiation of mesenchymal stem cells. *PLoS One* **3**, e3737, 2008.
- S32. Sundelacruz, S., Levin, M., and Kaplan, D.L. Depolarization alters phenotype, maintains plasticity of predifferentiated mesenchymal stem cells. *Tissue Eng Pt A* **19**, 1889, 2013.
- S33. Sundelacruz, S., Levin, M., and Kaplan, D.L. Comparison of the depolarization response of human mesenchymal stem cells from different donors. *Sci Rep-Uk* **5**, Article number: 18279, 2015.
- S34. Sundelacruz, S., Li, C.M., Choi, Y.J., Levin, M., and Kaplan, D.L. Bioelectric modulation of wound healing in a 3D in vitro model of tissue-engineered bone. *Biomaterials* **34**, 6695, 2013.
- S35. Eil, R., Vodnala, S.K., Clever, D., *et al.* Ionic immune suppression within the tumour microenvironment limits T cell effector function. *Nature* **537**, 539, 2016.
- S36. Jo, C.H., Lee, Y.G., Shin, W.H., *et al.* Intra-articular injection of mesenchymal stem cells for the treatment of osteoarthritis of the knee: a proof-of-concept clinical trial. *Stem Cells* **32**, 1254, 2014.
- S37. Orozco, L., Munar, A., Soler, R., *et al.* Treatment of knee osteoarthritis with autologous mesenchymal stem cells: two-year follow-up results. *Transplantation* **97**, e66, 2014.
- S38. McCrum, C. Therapeutic Review of Methylprednisolone Acetate Intra-Articular Injection in the Management of Osteoarthritis of the Knee - Part 2: Clinical and Procedural Considerations. *Musculoskelet Care* **14**, 252, 2016.
- S39. Ayhan, E., Kesmezacar, H., and Akgun, I. Intraarticular injections (corticosteroid, hyaluronic acid, platelet rich plasma) for the knee osteoarthritis. *World J Orthop* **5**, 351, 2014.
- S40. Kristjansson, B., and Honsawek, S. Current trends of stem cell-based approaches for knee osteoarthritis. *OA Tissue Eng* **1**, 7, 2013.
- S41. Gait, A.D., Hodgson, R., Parkes, M.J., *et al.* Synovial volume vs synovial measurements from dynamic contrast enhanced MRI as measures of response in osteoarthritis. *Osteoarthritis Cartilage* **24**, 1392, 2016.
- S42. O'Neill, T.W., Parkes, M.J., Maricar, N., *et al.* Synovial tissue volume: a treatment target in knee osteoarthritis (OA). *Ann Rheum Dis* **75**, 84, 2016.
- S43. Pessler, F., Chen, L.X., Dai, L., *et al.* A histomorphometric analysis of synovial biopsies from individuals with Gulf War Veterans' Illness and joint pain compared to normal and osteoarthritis synovium. *Clin Rheumatol* **27**, 1127, 2008.

- S44. Caron, J.P., Gandy, J.C., Schmidt, M., Hauptman, J.G., and Sordillo, L.M. Influence of corticosteroids on interleukin-1 beta-stimulated equine chondrocyte gene expression. *Vet Surg* **42**, 231, 2013.
- S45. Doyle, A.J., Stewart, A.A., Constable, P.D., Eurell, J.A.C., Freeman, D.E., and Griffon, D.J. Effects of sodium hyaluronate and methylprednisolone acetate on proteoglycan synthesis in equine articular cartilage explants. *Am J Vet Res* **66**, 48, 2005.
- S46. Frankenberger, M., Haussinger, K., and Ziegler-Heitbrock, L. Liposomal methylprednisolone differentially regulates the expression of TNF and IL-10 in human alveolar macrophages. *Int Immunopharmacol* **5**, 289, 2005.
- S47. Torheim, E.A., Yndestad, A., Bjerkeli, V., Halvorsen, B., Aukrust, P., and Froland, S.S. Increased expression of chemokines in patients with Wegener's granulomatosis - modulating effects of methylprednisolone in vitro. *Clin Exp Immunol* **140**, 376, 2005.
- S48. Barton, K.I., Heard, B.J., Chung, M., *et al.* Location and gene-specific effects of methylprednisolone acetate on mitigating IL1beta-induced inflammation in mature ovine explant knee tissue. *Inflamm Res* **66**, 239, 2017.